12

Thermodynamic evaluation of a combined ORC-TFC cycle for power generation from low-grade energy sources

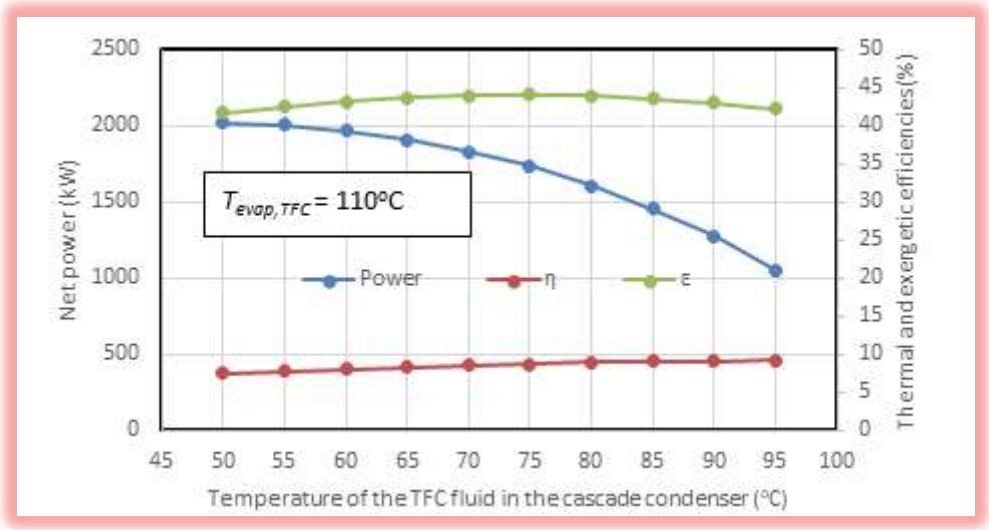

This chapter presents a new power generation cycle for utilising low-grade and renewable energy sources that combines the Organic Rankine Cycle (ORC) with the Trilateral Flash Cycle (TFC). By connecting the two cycles via a cascade condenser and applying the TFC in the high-temperature circuit, the combined cycle enjoys the merits of each cycle while minimising its drawbacks. The thermodynamic performance of the cycle is evaluated by using an Excel-based model that determines the fluid properties with Thermax functions for the refrigerants' group. The accuracy of these functions is first checked by comparing their estimations with relevant published data for the basic ORC and TFC cycles with a number of relevant fluids. The performance of the combined cycle with hot water at 120°C is compared to those of the simple TFC and ORC by using R152a as the working fluid in all three cycles. It is also compared to those of other two-stage and combined ORC-TFC cycles for a source temperature at 300°C using R234fa in the ORC circuit and water in the TFC circuit. Finally, the cycle is analysed with five fluids of low GWP, which are R1234yf in the ORC and R152a, R600, R600a, or R717 in the TFC. The performance of the best pair found, which is R152a/R1234yf, is compared with that of R152a as the single fluid at the cascade temperature that simultaneously maximises the cycle's power, thermal efficiency, and exergetic efficiency.

12.1. Literature review

Fossil-fuels are still the primary source of energy for electricity generation in both developed and developing countries. However, the mounting concerns about the damage to the environment and the climate changes have inspired intensive research for utilising renewable energy sources such as solar and geothermal energies. Another abundant source of energy that can also contribute to solving this problem is the wasted heat in the industrial, commercial, and transport sectors [1-3]. A common feature of these two energies is their low to moderate temperatures. Therefore, the development of appropriate technologies for utilising low/moderate energy sources is beneficial to both. In this respect, one of the promising technologies are the power generation systems that apply the ORC. Unlike the conventional Rankine cycle that requires steam at very high temperatures to drive the turbine, the ORC can be adapted to heat sources at low and moderate temperatures by using an organic working fluid instead of water. Low efficiency is the main drawback of the cycle particularly for the low-temperature (<100°C) energy sources that constitute 63% of the waste heat [4]. According to Iqbal et al. [5], the simple ORC is not economically feasible at temperatures lower than 80°C.

As for the conventional Rankine cycle, various improvements to the simple ORC have been considered such as reheating, regeneration, and recuperation [2]. However, such modifications do not address an inherent drawback of the cycle which is the mismatch between the temperature of the heating source and that of the working-fluid during the heat-addition process in the evaporator since the first remains constant while the second drops steadily. To solve this problem, the TFC has been proposed [5-9]. In this cycle, the heat recovery process is not allowed to vaporise the working which is taken directly as saturated liquid to expand in a two-phase expander. The problem with the TFC is that the technology of expanders is relatively immature and, therefore, they are less efficient

compared to the conventional turbines [2]. According to various researchers, the two-phase expander is the main factor for degrading the efficiency of the TFC [6 - 8].

Many previous studies dealt with theoretical analyses for evaluating the performance of the ORC and TFC from thermodynamics and thermo-economic viewpoints. For example, Bidgoli and Yanagihara [1] analysed an ORC system to recover the waste heat from the intercoolers of the compression units of a large processing plant. By using Aspen HYSYS, they compared the cycle's performance with various working fluids including R123, n-butane, n-pentane, hexane, and n-heptane. Their results showed that a net power of up to 40 MW could be generated with R123. Wolf et al. [3] investigated a solar powered ORC using pure iso-pentane and two iso-pentane/CO_2 zeotropic mixtures. Modelling of the system was done by using EES (Engineering Equation Solver) and the thermodynamic properties were determined by using REFPROP. Their exergy and exergo-economic analyses showed that the investigated unit was capable of co-producing approximately 30 kW electricity and 160 kW district heating with an exergetic efficiency exceeding 60%. Therefore, they concluded that the unit was able to compete with existing renewable power generating systems in terms of specific cost of electricity.

Yari et al. [7] compared the ORC and TFC cycles for a 120^{o}C low-grade heat source. They conducted parametric studies for several working fluids in the two cycles by using EES. Their results showed that increasing the inlet temperature of the TFC expander will increase the net output power and decreases the product cost, but this was not the case for the ORC system. Although the TFC could achieve a higher net output power compared with the ORC system, they found that its product cost was greatly affected by the expander's isentropic efficiency. Lykas et al. [9] compared two options for utilising the same low-temperature (80-100^{o}C) heat source. The first option was an ORC in which a small fraction of the supplied waste heat was continuously provided to the expander with the aim of approaching a quasi-isothermal process and the second option was the TFC. They performed parametric thermodynamic analyses of the two cycles, with R1234ze(E), R1234yf, R1233zd(E), and R134a as working fluids by using Aspen Plus software. Their techno-economic study of the first cycle with the four working fluids showed that R1233zd(E) was the most proper working fluid for the cycle.

More recent studies considered the use of a two-stage ORC (also called dual-loop ORC) for relatively high-temperature sources such as the exhaust gas of diesel engines [10-12] or geothermal energy [13]. This cycle enables different organic fluids to be used in the high-temperature circuit (HTC) and low-temperature circuit (LTC) that suit the high and low temperature ranges better than a single fluid. For such high-temperature sources also, Li et. al. [14] and Yu et. al. [15] presented a combined cycle that applies the TFC in the HTC and the ORC in the LTC. The working process of the proposed system is similar to that of the dual-loop ORC, but the use of a TFC instead of an ORC in the HTC minimises the mismatch between the working fluid and the heat source. To determine the fluids' thermodynamic properties, they used the REFPROP software. By comparing the cycle's performance with that of the conventional dual-loop ORC for an exhaust gas at 300^{o}C by

using R245fa in the LTC and cyclohexane, toluene, benzene, octane, and water in the HTC, Yu et. al. [15] showed that the combined TFC-ORC cycle offers a better thermodynamic performance than that of the conventional dual-loop ORC.

The few examples given above represent the numerous research efforts made in the past that investigated the use of ORC and TFC for utilising low-grade energy sources. These, and the more comprehensive review given by Jiménez-García et al [16], indicate that the combined ORC-TFC cycle has not been adequately evaluated particularly for the lowest-temperature energy sources (<140°C). In this regard, this study presents a thermodynamic evaluation of a new combined ORC-TFC cycle that is designed for this type of energy sources. From another perspective, the literature review shows that most researchers used commercial software for their analyses. However, the use of general-purpose software can encourage independent researchers and engineering students to contribute to the development of innovative systems for the utilisation of renewable and low-grade energy sources [17, 18]. In this respect, the present study uses Microsoft Excel as the modelling platform with special VBA functions to determine the thermodynamic properties of the working fluids, Excel solver for the single-objective optimisation analyses, and the free version of the MIDACO solver [19] for the multi-objective optimisation analyses.

12.2. The simple ORC and TFC

Figure 12.1 shows schematic diagrams of the simple ORC and TFC systems and Figure 12.2 shows their respective *T-s* diagrams. As Figure 12.1.a shows, the ORC system has the same components as those of the conventional steam-turbine power plant. Organic fluids are used in the ORC instead of water because they have higher boiling pressures at lower temperatures and, therefore, suit the low-temperature applications better. To avoid the problem of blade erosion at the last turbine stages, dry or isentropic fluids for which the saturated liquid-vapour curves have negative or infinite slopes, respectively, are usually selected [2,20].

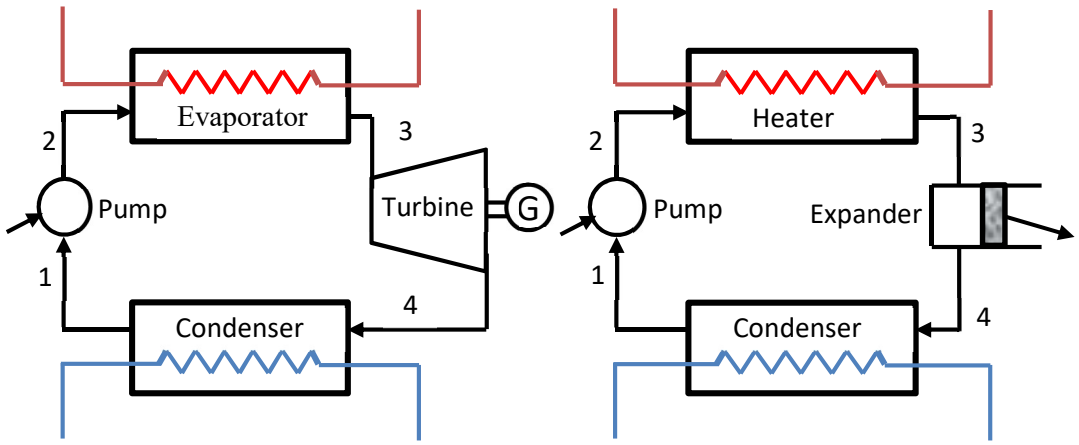

(a) (b)

Figure 12.1. Schematic diagrams of: (a) the ORC system and (b) the TFC system

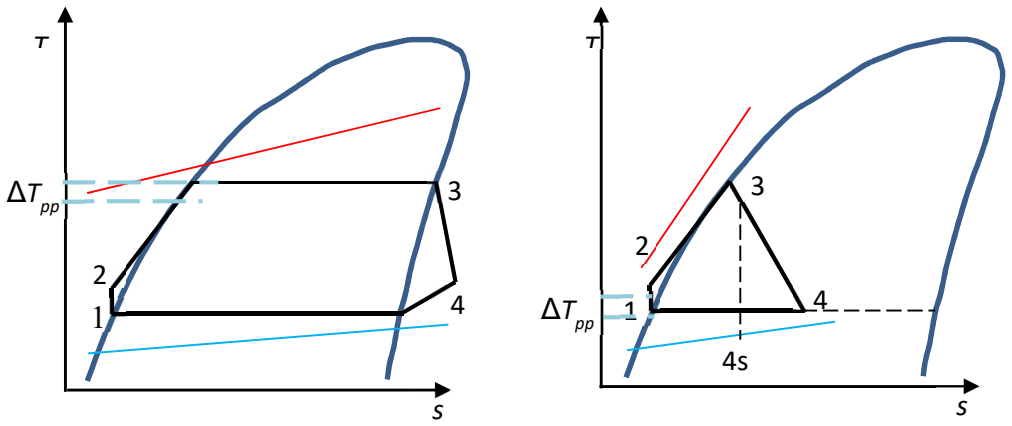

(a) (b)

Figure 12.2. *T-s* diagrams of: (a) the ORC cycle and (b) the TFC cycle

The TFC system also uses organic fluids, but differs from the ORC in that it heats the working fluid without going into the vaporisation process so that the saturated pressurised liquid expands in the two-phase region. As Figure 12.2.b shows, the TFC leads to a uniform temperature glide between the heat source and the working fluid; which reduces the losses during the heat-transfer process and improves the performance of the system. Typically, TFC systems can provide 50% more work than ORC systems for the same energy input, but they need sophisticated expanders that can adequately handle the liquid-phase presence during the expansion process [2]. Apart from increasing the investment cost, two-phase expanders are generally less efficient and have limited compression ratios compared to conventional vapour turbines. This section describes the analytical models for thermodynamic analyses of the two cycles and their implementation by using Excel.

12.2.1. The analytical model for the TFC

The analytical model for the TFC neglects pressure losses and heat-transfer losses in the various components, but takes into consideration the losses due to irreversibility in the pump and the two-phase expander via the relevant isentropic efficiencies [21]. Given the inlet temperature of the heat source, $T_{hs,in}$, and its mass flow rate, $\dot{m}_{hs}$, the rate of heat transfer from the heat source (a stream of hot-water) to the working fluid of the TFC, $\dot{Q}_{hs,TFC}$, and the mass flow rate of the working fluid, $\dot{m}_{TFC}$, are calculated from:

$$\dot{Q}_{hs,TFC} = \dot{m}_{hs} c_p \left(T_{hs,in} - T_{hso,TFC}\right) \tag{12.1}$$

$$\dot{m}_{TFC} = \dot{Q}_{hs,TFC} / \left(h_3 - h_2\right) \tag{12.2}$$

The temperature of the heat source exiting the heater of the TFC, $T_{hso,TFC}$, is determined given the pinch-point temperature difference, ΔT_{pp}, from:

$$T_{hso,TFC} = T_2 + \Delta T_{pp} \tag{12.3}$$

The enthalpy at state 3 is taken as that of saturated liquid at the evaporator pressure. The enthalpy of the fluid at state 2 after the pump is determined from:

$$h_2 = h_1 + w_{p,TFC} \tag{12.4}$$

Where h_1 is the enthalpy at point 1, which is taken as that of saturated liquid at the condenser pressure, and $w_{p,TFC}$ is the TFC pump specific work given by:

$$w_{p,TFC} = v_1\left(p_{eva,TFC} - p_{cc,TFC}\right)/\eta_{p,TFC} \tag{12.5}$$

Where $p_{eva,TFC}$ and $p_{cc,TFC}$ are the pressures of the TFC fluid in the evaporator and condenser, respectively. The specific work, in kJ per kg, of the working fluid during the two-phase expansion process is evaluated from the enthalpy change as follows:

$$w_{exp} = \left(h_3 - h_{4s}\right) \times \eta_{exp} \tag{12.6}$$

Where η_{exp} is the isentropic efficiency of the expander and h_{4s} is the enthalpy of the fluid after an isentropic expansion. The thermal efficiency of the TFC is given by:

$$\eta_{TFC} = \dot{m}_{TFC}\left(w_{exp} - w_{p,TFC}\right)/\dot{Q}_{hs,TFC} \tag{12.7}$$

Lai et al. [8] analysed the performance of a TFC system with the following input data:

- The heat source = 80ºC,
- The mass flow rate of the heat source = 4.16 kg/s,
- The heat sink temperature = 30ºC,
- The fluid's inlet temperature to the condenser = 37ºC,
- The isentropic efficiency of the pump = 0.7.

For their analyses, they selected four working fluids, which are R134a, R236fa, R245fa, and R1233zd. The present analysis involves only R134a, R245fa, and R1233zd because R236fa is not supported by Thermax. Figure 12.3 shows the model developed for the cycle using the input data shown above. While Lai et al. [8] fixed the temperature T_2 at 35ºC, in the present analysis T_2 is not fixed but evaluated by the model. Figure 12.3 shows the calculated value of T_2 as 37.8ºC. Figure 12.4 shows the results obtained by the reference model that determined their thermodynamic properties by using the REFPROP, while Figure 12.5 shows those of the present model for the cycle's power and thermal efficiency. The two figures show a close agreement and both figures show that R134a has considerably lower values than those of R236fa and R1233zd.

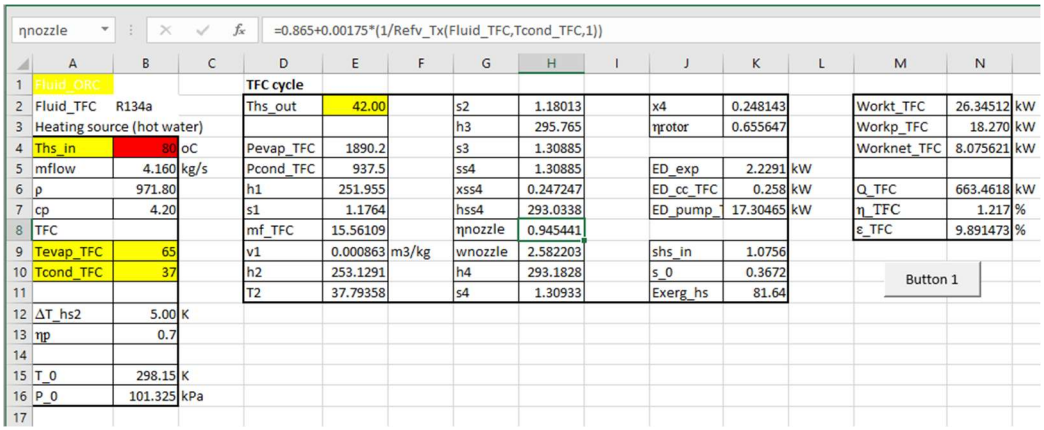

	A	B	C	D	E	F	G	H	I	J	K	L	M	N	
1	Fluid_ORC			TFC cycle											
2	Fluid_TFC	R134a		Ths_out	42.00		s2	1.18013		x4	0.248143		Workt_TFC	26.34512	kW
3	Heating source (hot water)						h3	295.765		ηrotor	0.655647		Workp_TFC	18.270	kW
4	Ths_in	80	oC	Pevap_TFC	1890.2		s3	1.30885					Worknet_TFC	8.075621	kW
5	mflow	4.160	kg/s	Pcond_TFC	937.5		ss4	1.30885		ED_exp	2.2291	kW			
6	ρ	971.80		h1	251.955		xss4	0.247247		ED_cc_TFC	0.258	kW	Q_TFC	663.4618	kW
7	cp	4.20		s1	1.1764		hss4	293.0338		ED_pump_1	17.30465	kW	η_TFC	1.217	%
8	TFC			mf_TFC	15.56109		ηnozzle	0.945441					ε_TFC	9.891473	%
9	Tevap_TFC	65		v1	0.000863	m3/kg	wnozzle	2.582203		shs_in	1.0756				
10	Tcond_TFC	37		h2	253.1291		h4	293.1828		s_0	0.3672		Button 1		
11				T2	37.79358		s4	1.30933		Exerg_hs	81.64				
12	ΔT_hs2	5.00	K												
13	ηp	0.7													
14															
15	T_0	298.15	K												
16	P_0	101.325	kPa												
17															

Figure 12.3. The Excel-aided model for the TFC using R134a with the data of [8]

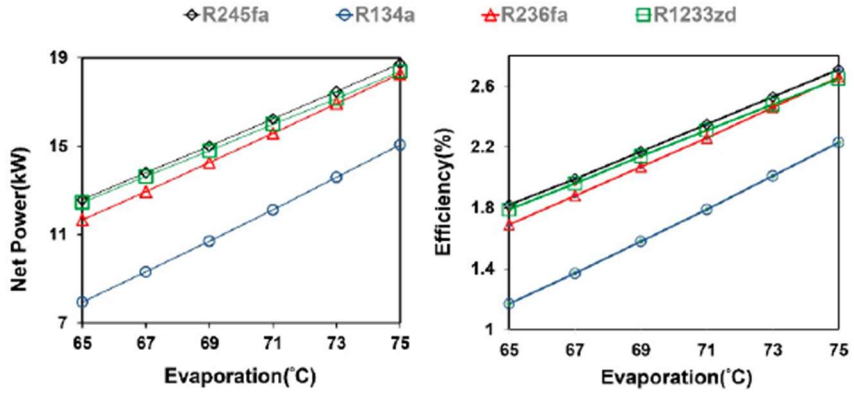

(a) (b)

Figure 12.4. Variations of (a) the net power and (b) thermal efficiency of the TFC with the evaporation temperature as given by Lai et al. [8]

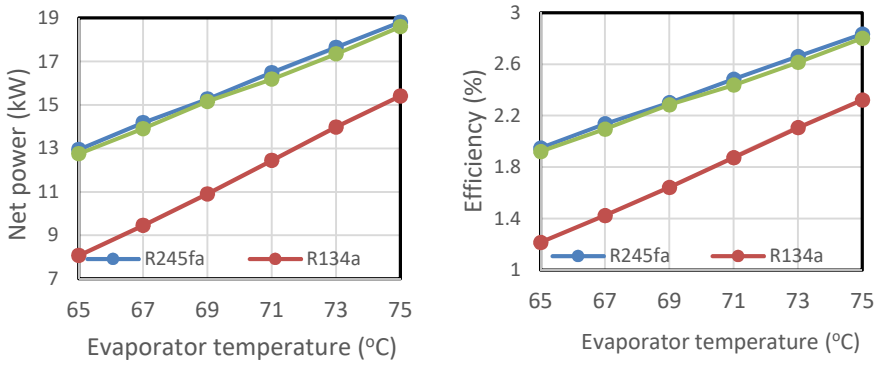

(a) (b)

Figure 12.5. Variations of (a) the net power and (b) thermal efficiency of the TFC with the evaporation temperature as obtained by the present model

12.2.2. The analytical model for the ORC

This model is based on the same assumptions made for the TFC model. The pump specific work is given by:

$$w_{p,ORC} = v_1\left(p_{cc,ORC} - p_{con,ORC}\right)/\eta_{p,ORC} \tag{12.8}$$

Where $\eta_{p,ORC}$ is the isentropic efficiency of the ORC pump.

The enthalpy at point 1 is taken as that of saturated liquid at the condenser pressure, while that at state 3 is taken as that of saturated vapour at the evaporator pressure. The enthalpy h_4 is determined by allowing for the irreversibility of the turbine as follows:

$$h_4 = h_3 + \left(h_3 - h_{4s}\right)\times\eta_t \tag{12.9}$$

Where h_{4s} is the enthalpy after an isentropic expansion and η_t is the isentropic efficiency of the turbine. The turbine's specific work is then calculated from:

$$w_t = h_3 - h_4 \tag{12.10}$$

The thermal efficiency of the ORC is given by:

$$\eta_{ORC} = \dot{m}_{ORC}\left(w_t - w_{p,ORC}\right)/\dot{Q}_{hs,TFC} \tag{12.11}$$

Where $\dot{Q}_{hs,ORC}$ is the heat recovered in the ORC, which is given by:

$$\dot{Q}_{hs,ORC} = \dot{m}_{ORC}\left(h_3 - h_2\right) \tag{12.12}$$

Yari et al. [7] analysed the simple ORC with a heat source at 120ºC with seven working fluids, which are: R134a, R1234yf and R152a, propane (R290), n-butane (R600), iso-butane (R600a), and ammonia (R717). Their input data are shown on Table 12.1.

Table 12.1. Values of the parameters used for validating the simple ORC model [7]

Parameter	Value
T_{hs} (ºC)	120
$\dot{m}_{hs}$ (kg/s)	100
T_{cond} (ºC)	40
ΔT_{pp} (K)	10
η_p (%)	85
η_t (%)	85

Figure 12.6 shows the Excel-aided model developed for verifying Thermax property functions for this cycle by comparing their results with those obtained by Yari et al. [7]. The sheet consists of four blocks of cells. The first block on the left side of the sheet stores the specified data, while the second and third blocks in the middle perform the calculations required by the analytical model. The fourth block on the right side of the sheet determines the overall cycle parameters that include the total amount of recovered heat (Qhs_tot), the net power produced by the system (Work_net), the exit temperature of the heating source (Ths_out), and the overall energetic (therm_eff) and exergetic (exg_eff) efficiencies. The sheet uses R152a as the working fluid, but the name of the fluid is stored as a variable "Fluid" so that it can be used for other working fluids.

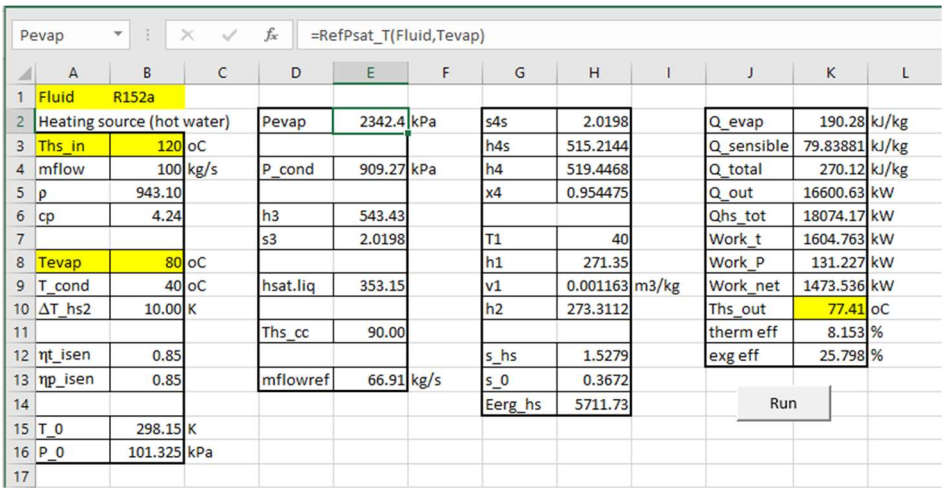

Figure 12.6. The Excel-aided model for the simple ORC with the data given by [7]

The system's power output, thermal efficiency, and exergetic efficiency were calculated at various values of the turbine's inlet temperature, T_3, which is also the temperature of the working fluid in the evaporator, for the seven working fluids. The "Run" button shown in Figure 12.6 is linked to a macro that records the model's calculations for the first fluid so that the same calculations can easily be repeated for the other fluids. The results obtained by the present model are compared on Figures 12.7 and 12.8 with those obtained by Yari et al [7] who also used EES to develop their model. The two figures show close agreement between the results of the present model and their model.

12.3. The proposed combined ORC- TFC cycle

Figures 12.7 and Figure 12.8 show that both the power output and thermal efficiency of the simple ORC drop at evaporator temperatures higher than 80ºC with four of the analysed fluids. The other three fluids, R134a, R1234yf, and R290, yield the highest power and thermal efficiency at the lower end of the temperature, but they cannot be used higher than 85-95ºC because of their critical temperature limits. The power and thermal efficiency of the simple ORC also drop at temperatures lower than 75ºC. Since the TFC cannot cover the whole range of temperatures because of its pressure ratio limitation,

combining the two cycles with each one covering part of the temperature span appears to be a sensible solution. Figure 12.9 shows schematic and *T-s* diagrams of a system in which the heat source is first used to heat the working fluid of the TFC circuit and then heat the working fluid of the ORC circuit. After expanding in the two-phase expander, the working fluid of the TFC circuit is condensed by the cooler working fluid of the ORC circuit in a cascade condenser (cc) before being pumped into the TFC heater.

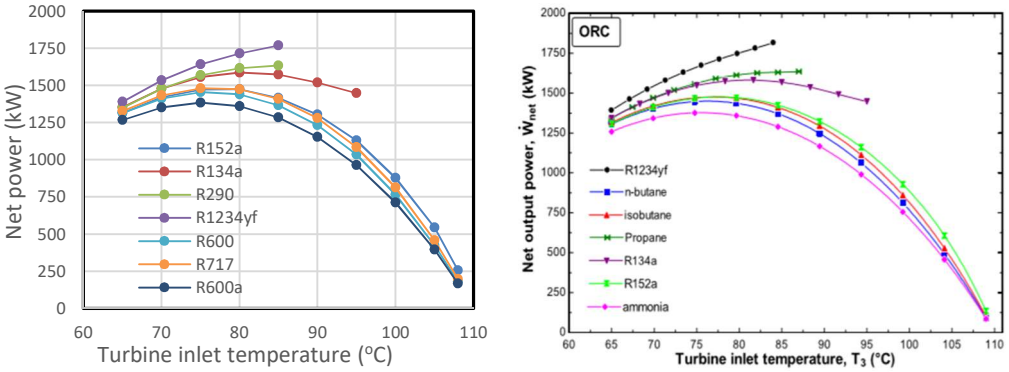

(a) (b)

Figure 12.7. Comparison of (a) the model's estimations for the net power of the ORC at various values of T_3 with (b) the reference [7]

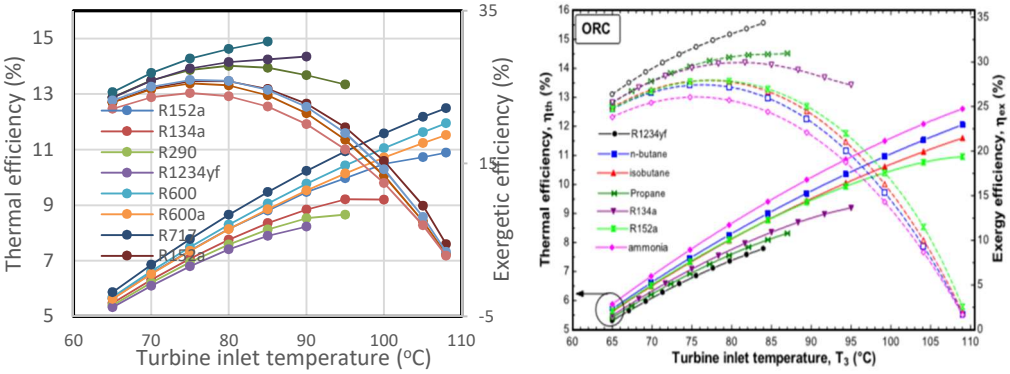

(a) (b)

Figure 12.8. Comparison of (a) the model's estimations for thermal efficiency and exergetic efficiency of the ORC at various values of T_3 with (b) the reference [7]

The ORC system shown on Figure 12.9.a is a recuperative system in which the superheated fluid exiting the turbine is used to heat the cold fluid exiting the pump in an internal heat-exchanger (IHEX). In the condenser, the working fluid is cooled by the cold-sink fluid to the saturated-liquid state and then pumped into the cold side of the IHEX to be heated by the heat source to the state of saturated liquid before entering the cascade condenser where it is heated further by the condensing fluid of the TFC circuit until it becomes saturated vapour and then expanded in the ORC turbine.

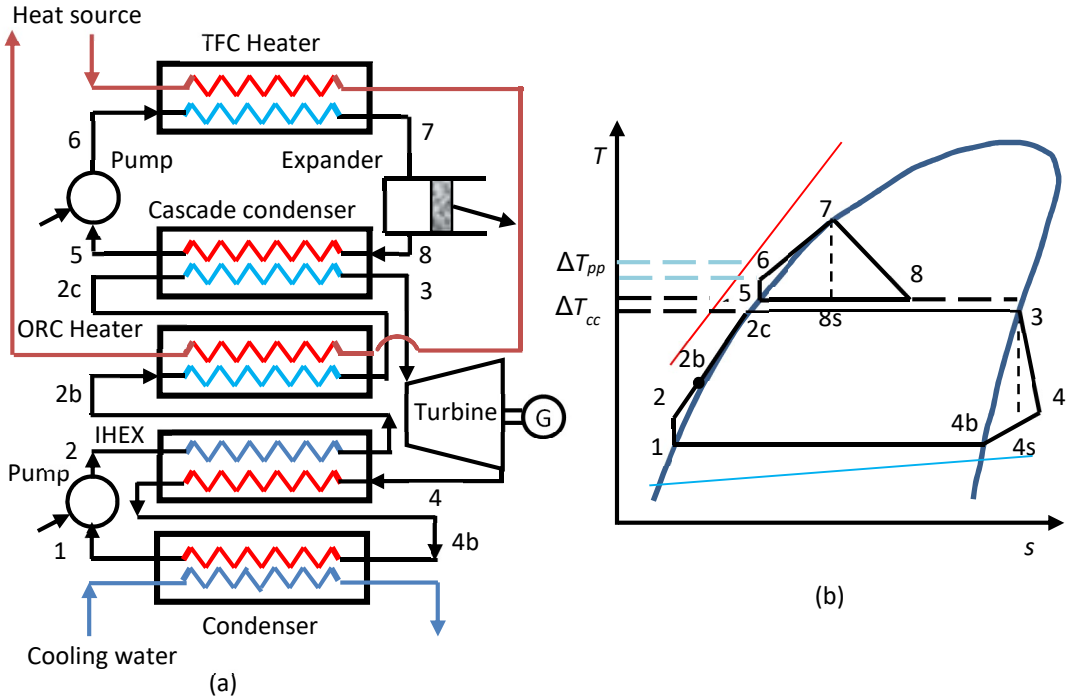

Figure 12.9. Schematic and *T-s* diagrams for the combined ORC-TFC cycle with the same working fluid in the ORC and TFC

Unlike the TFC cycle in which the pinch point occurs where the heating fluid exits the system, for this cycle Figure 12.9.b shows that the pinch point occurs in the middle of the heating process. Although this forces the heating source to exit the system at a relatively high temperature and limits the amount of heat recovered and the work produced by the ORC circuit, the combined cycle can still produce more work than the simple ORC alone because of the additional work produced by the TFC. Compared to a simple TFC, the combined cycle may not be able to produce the same power, but it can have a higher thermal efficiency by replacing the two-phase expander with the single-phase turbine in the ORC circuit and by allowing two different working fluids to be used in the TFC and ORC circuits leading to a better overall performance than a single fluid. Three of the seven fluids considered by Yari et al [7] can be used in the ORC, while the other four can be used in the TFC. Compared to the system described by Yu et al. [15], in this system the heat transfer from the TFC fluid to the ORC fluid occurs isothermally and that from the heating source to the ORC fluid does not involve phase change (vaporisation). Therefore, this system gives a better match between the temperature profiles of the fluids involved. Moreover, the ORC includes a heat-exchanger for preheating the ORC fluid.

12.3.1. The analytical model for the combined cycle

Referring to Figure 12.9b, the mass flow rates of the working fluids in the ORC and TFC circuits are related by:

$$\dot{m}_{ORC} = \dot{m}_{TFC}\left(h_8 - h_5\right)/\left(h_3 - h_{2c}\right) \tag{12.8}$$

The total heat recovered from the heat source and total net power produced by the combined cycle, respectively, are given by:

$$\dot{Q}_{hs,tot} = \dot{Q}_{hs,TFC} + \dot{Q}_{hs,ORC} \tag{12.15}$$

$$\dot{W}_{tot} = \dot{m}_{ORC}\left(w_t - w_{p,ORC}\right) + \dot{m}_{TFC}\left(w_{exp} - w_{p,TFC}\right) \tag{12.16}$$

The overall thermal efficiency and exergetic efficiency of the cycle are given by:

$$\eta_{tot} = \dot{W}_{tot} / \dot{Q}_{hs,tot} \tag{12.17}$$

$$\varepsilon_{tot} = \dot{W}_{tot} / \dot{E}_{hs,in} \tag{12.18}$$

Where $\dot{E}_{hs,in}$ in Equation (12.18) is the rate of exergy flow of the heat source entering the system defined as [7]:

$$\dot{E}_{hs,in} = \dot{m}_{hs}\left[\left(h_{hs,in} - h_0\right) - T_0\left(s_{hs,in} - s_0\right)\right] \tag{12.19}$$

Finally, the temperature of the heat source exiting the system is given by:

$$T_{hs,out} = T_{hs,in} - \dot{Q}_{hs,tot} / \dot{m}_{hs} c_p \tag{12.20}$$

Where c_p is the specific heat of the heating medium.

12.3.2. The Excel model for the combined cycle

Figure 12.10 shows the model developed for the combined cycle in which the first block of cells on the left side of the sheet stores the specified data, while the second and third blocks in the middle perform the calculations for the TFC and ORC circuits, respectively. The fourth block on the right side of the sheet determines the overall cycle parameters. The names of the working fluids in the TFC and ORC circuits are stored as variables so that the model can be used for different fluid pairs, but the model shown on Figure 12.10 uses R152a in both circuits. The cascade-condenser temperature difference is taken as 3ºC. Figure 12.10 shows that the temperature of the TFC fluid in the cascade condenser, Tcc_TFC, and that of the ORC fluid, Tcc_ORC, are specified as 83ºC and 80ºC, respectively. By fixing value of the temperature of the TFC fluid entering the expander at 110ºC, the power, thermal efficiency, and exergetic efficiency of the combined cycle

were calculated at various values of the cascade-condenser temperature in the cycle with R152a as the single working fluid. The results are plotted on Figure 12.11.

Pevap_TFC =RefPsat_T(Fluid_TFC,Tevap_TFC)

	A	B	C	D	E	F	G	H	I	J	K	L	M	N	O
1	**Working fluids**			**TFC cycle**									**TFC**		
2	Fluid_TFC	R152a		T_hsi	93.00		s6	1.508015		h8	434.86189		Workt_TFC	656.4599	kW
3	Fluid_ORC	R152a					h7	439.22		s8	1.7098828		Workp_TFC	433.9989	kW
4	**Heating source (hot water)**			Pevap_TFC	4243.2		s7	1.7058					Worknet_TFC	222.4611	kW
5	T_hs	120	oC	Pcc_TFC	2503.08								Q_TFC	11458.8	kW
6	mflow	100	kg/s	h5	360.266		ss8	1.7058					η_TFC	1.941	%
7	ρ	943.10	kg/m3	s5	1.50023		xss8	0.40023							
8	cp	4.24	kJ/kg.K	mf_TFC	150.62947		hss8	433.4092		s_hs	1.5279		**ORC**		
9	**TFC**			v5	0.0014074	m3/kg				s_0	0.3672		Q_sensible	91.67203	kJ/kg
10	Tevap_TFC	110	oC	h6	363.1472					Exerg_hs	3472.92		Q_ORC	5413.38	kW
11	Tcc_TFC	83	oC	T6	84.214554								Workt_ORC	1416.248	kW
12	ΔTcc	3	K	**ORC cycle**									Workp_ORC	115.811	kW
13	ΔT_hs2	10	K	Tcc_ORC	80	oC	s4s	2.0198		h2	273.31119		Worknet_ORC	1300.436	kW
14	**ORC**			Pcc_ORC	2342.4	kPa	h4s	515.2144		T2	41.037827		η_ORC	7.811	%
15	Tcond_ORC	40	oC	Pcond_ORC	909.27	kPa	h4	519.4468		s2	1.2472232				
16	ΔT_sc	0.00	K				T4	40					**Overall parameters**		
17	ηt_isen	0.85		h3	543.43		s4	2.033315		h2b	261.47797		Q_total	16872.18	kW
18	ηp_isen	0.85		s3	2.0198					T2b	34.724121	kJ/kg	T_hsout	80.24	oC
19	ηx_isen	0.75		h2c	353.15		T1	40	oC	s2b	1.2098085	kg/s	Q_out	15349.28	kW
20	T_0	298.15	K	s2c	1.481		h1	271.35	kJ/kg						
21	P_0	101.325	kPa				v1	0.001163	m3/kg	Qevap_ORC	190.28	kW	W_total	1522.897	kW
22				h4b	531.28		s1	1.2411		mf_ORC	59.05	kW	η_overall	9.026	%
23				s4b	2.0711								ε_overall	43.85063	%
24															

Figure 12.10. Excel-aided model for the combined cycle using R152a with the data shown on Table 12.1

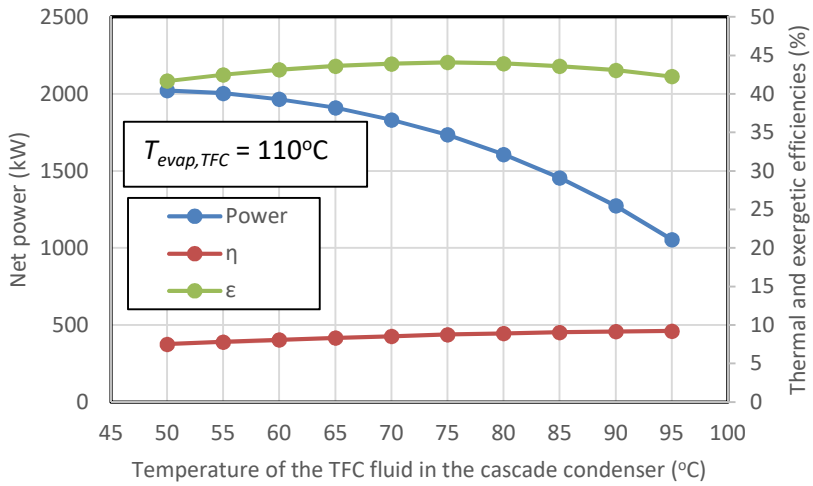

Figure 12.11. Variation of the combined-cycle's power and thermal and exergetic efficiencies with the temperature of the TFC fluid in the cascade condenser

Figure 12.11 shows that the thermal efficiency of the combined cycle increases steadily with the temperature of the ORC fluid in the cascade condenser, but its power drops while the exergetic efficiency has a maximum value at the cascade temperature of 75°C. Clearly, the cascade temperature has to selected such that it gives the required trade-off between the cycle's produced power, thermal efficiency, and exergetic efficiency.

12.4. Comparison with the ORC and TFC using R152a only

In this section, the performance of the combined cycle will be compared to those of the simple ORC and TFC using R152a as the working fluid for all three cycles with the data shown on Table 12.1. For the TFC, the model shown on Figure 12.7 had to be modified and Figure 12.12 shows the modified model with R152a as the working fluid and using the input data of Table 12.1. For both the TFC and the combined cycle, the temperature of the TFC fluid entering the TFC expander was taken as 110°C and the isentropic efficiency of the TFC expander was specified as 75%. Also note that the condenser temperature for the TFC is now 40°C and the pinch-point temperature difference is 10°C. For the ORC, Figures 12.5 shows that the cycle has a certain temperature in its evaporator that maximises its output power, which is 80°C. Therefore, the comparison with the ORC will be based on the cycle's performance at this temperature as shown on Figure 12.4.

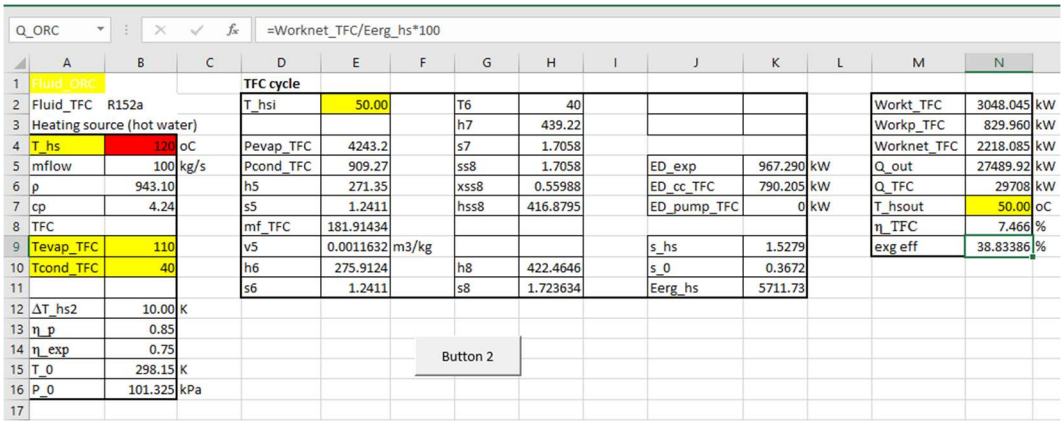

Figure 12.12. The modified model for the TFC cycle with R152a as the working fluid

Table 12.2 compares the values obtained by the three cycles for a number of performance indicators. For the ORC and TFC cycles, the relevant values are obtained from Figure 12.6 and Figure 12.12, respectively. For the combined cycle, three sets of values are shown which correspond to three values of the temperature of the ORC fluid in the cascade condenser, Tcc_ORC, which are 70°C (CC-70), 80°C (CC-80), and 90°C (CC-90). The table figures show that the lowest exit temperature for the heat source is that of the TFC, which is 50°C, and the highest exit temperature is that of the combined cycle CC_90, which is 90.72°C.

Table 12.2. Performance parameters of the ORC, TFC, and the combined cycle

	TFC	ORC	CC-70	CC-80	CC-90
Ths,out (°C)	50	77.41	71.75	80.24	90.72
Qin (kW)	29708	18074.17	20479.42	16872.18	12427.7
Qout (kW)	27489.92	16600.63	18700.75	15349.28	11278.86
Power (kW)	2218.085	1473.536	1778.665	1522.897	1148.837
Thermal efficiency (%)	7.466	8.153	8.685	9.026	9.244
Exergetic efficiency (%)	38.834	25.798	31.141	43.851	20.114

Figures 12.13 compares amount of heat recovered and power produced by the three cycles. The figure shows that the simple TFC recovers the most energy and produces the most power among the three cycles. The figure also shows that both the heat recovered and power produced by the combined cycle decrease as the cascade temperature is increased. The recovered energy and power produced by the combined cycle are lower than those of the TFC for all three cascade temperatures, but higher than that of the ORC for cascade temperatures of 80°C and below.

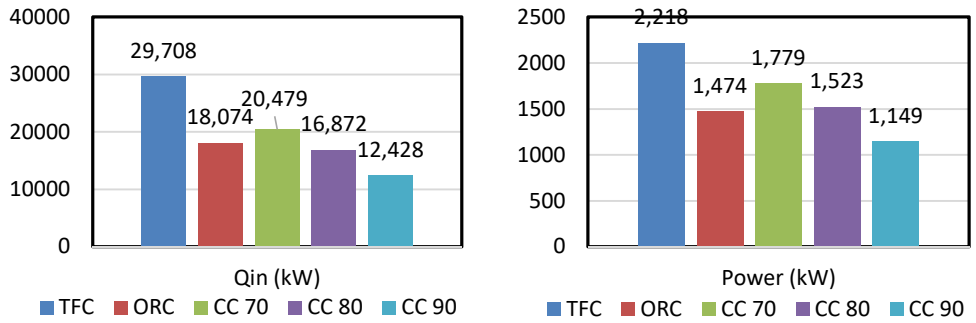

Figure 12.13. Comparison of the recovered heating source energy and power produced by the combined cycle with those of the simple TFC and ORC

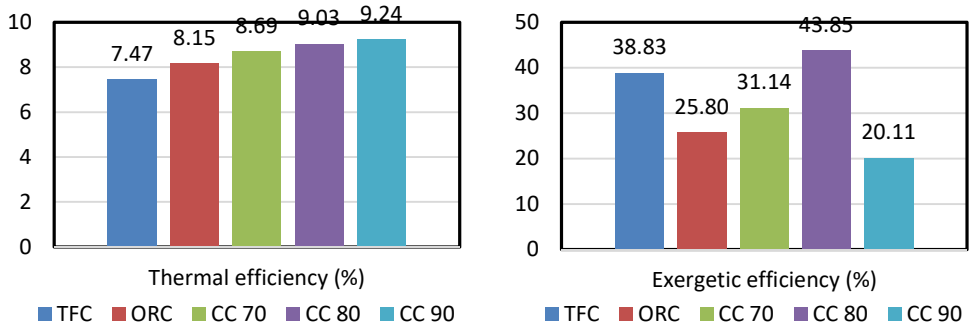

Figure 12.14. Comaprison of the and thermal efficiency and exergetic efficiency of the combined cycle with those of the simple TFC and ORC

An unconditional advantage of the combined cycle is revealed by Figure 12.14.a that compares its thermal efficiency and exergetic efficiency to those of the other two cycles. It shows that the thermal efficiency of the combined cycle is higher than those of the TFC and ORC at all three cascade temperatures and increases with the cascade temperature. Figure 12.14.b shows that the exergetic efficiency of the combined cycle at the cascade temperature of 80°C also exceeds those for both the simple TFC and ORC.

12.5. Comparison with other combined ORC-TFC cycles

To compare the present combined cycle with that described by Yu et al [15], it was applied to the case they considered that involved an exhaust gas at 300°C. Because of the

relatively high temperature of the gas, for the TFC circuit Yu et al [15] used cyclohexane, toluene, benzene, octane, and water. They studied the effects of the TFC evaporator temperature (T_{Evap_TFC}) on the performances of their system with these five working fluids in the HT circuit and R245fa in the LT circuit using the input data shown in Table 12.3.

Table 12.3. Input data for the combined-cycle analysis [15]

Parameters	Value and Unit
The inlet temperature of the exhaust	573 K (300°C)
The outlet temperature of the exhaust	383 K (110°C)
Mass flow rate of exhaust	804 kg/h (0.223 kg/s)
Condensing temperature of HT working fluid	358 K (85°C)
Condensing temperature of LT working fluid	308 K (35°C)
Evaporator pinch point temperature difference	30 K
Condenser pinch point temperature difference	10 K
Expander isentropic efficiency	0.85
Pump isentropic efficiency	0.65

Yu et al [15] used the REFPROP software to determine the thermodynamic properties of the fluids. Since Thermax group of functions do not cover cyclohexane, toluene, benzene, or octane, only water was used with present cycle. In order to avoid the condensation of water vapour in the exhaust gas, Yu et al [15] imposed a lower limit on the exhaust-gas temperature which is 110°C. However, this condition is difficult to apply with the present cycle since the energy required for the sensible heating of the LT fluid comes from the gas not the HT fluid. It should be mentioned that this lower limit won't be required when considering other low-grade energy sources with similar temperatures such as geothermal energy and industrial waste. Needless to say that not allowing energy source temperatures lower than 110°C makes the cycle useless for utilising the largest part of the low-grade energy sources which are available at 100°C and below. For these reasons, no lower limit was imposed on the exhaust-gas temperature in the present analysis.

Figure 12.15 shows the Excel sheet of the combined-cycle system with the necessary modifications to the data part. As the figure shows, the sheet uses R245fa as the working fluid in the ORC and R718 (water) as the fluid in the TFC. The figure shows that at T_{Evap_TFC} = 257°C and T_{Evap_ORC} = 70°C the net power produced by the system, thermal efficiency and exergetic efficiency are 10.36 kW, 20.22%, and 58.33%, respectively. By fixing T_{Evap_ORC} at 70°C, the three performance indicators were calculated by varying T_{Evap_TFC} from 167°C (440K) to 257°C (530K). Figures 12.16 to 12.18 compare the estimations of the present model with those obtained by Yu et al [15] using their combined cycle and a conventional dual-loop cycle with the same input data. The figures show that the net power, thermal efficiency, and exergetic efficiency of both combined cycles increase as T_{Evap_TFC} increases, while those of the conventional dual loop deteriorate as T_{Evap_TFC} is increased beyond 465K. The figures also show that the estimations of the present cycle agree well with those of the reference cycle both qualitatively and quantitatively with the present cycle showing slightly higher net power and exergetic efficiency and slightly lower thermal efficiency.

Tevap_ORC | =Tcond_TFC-ΔTcc

	A	B	C	D	E	F	G	H	I	J	K	L	M	N	O
1	Fluid_TFC	R718		TFC cycle			s6	1.91248		h8	987.6567		TFC		
2	Fluid_ORC	R245fa		T_hsi	110.00		s7	1120.12		s8	2.923674		Workt_TFC	7.22385	kW
3	Heating source (hot air)						h7	1120.12					Workp_TFC	0.3819	kW
4	T_hs	300	oC	Pevap_TFC	4470.66		s7	2.85748					Worknet_TFC	6.84198	kW
5	mflow	0.223	kg/s	Pcond_TFC	47.41		ss8	2.85748					Q_TFC	42.4333	kW
6	ρ	1.20		h5	335.01		xss8	0.27265					η_TFC	16.124	%
7	cp	1.00		s5	1.0756		hss8	964.28							
8	TFC			mf_TFC	0.054534								ORC		
9	Tevap_TFC	257		v5	0.001029	m3/kg				Δh_hs	236.38		Q_sensible	39.7424	
10	Tcond_TFC	80		h6	342.0125					Δs0_hs	0.53		Q_ORC	8.81794	
11	ΔTcc	10	oC	T6	157					ΔEerg_hs	17.77		Workt_ORC	3.62642	kW
12	ΔT_hs2	30	K	ORC cycle									Workp_ORC	0.104	kW
13				Tevap_ORC	70	oC	s4s	1.7736		h2	246.2718		Worknet_ORC	3.52284	kW
14	ORC			Pevap_ORC	609.6	kPa	h4s	435.771		T2	35.34576		η_ORC	7.933	%
15	Tcond_ORC	35	oC	Pcond_ORC	211.815	kPa	h4	438.656		s2	1.158821				
16	ΔT_sc	0.00	K				T4	43.6449					Overall parameters		
17	ηt_isen	0.85		h3	455		s4	1.78275		h2b	254.8476		Q_total	51.2513	kW
18	ηp_isen	0.65		s3	1.7736					T2b	41.67435	kJ/kg	T_hsout	70.52	oC
19	ηx_isen	0.85		hsat.liq	294.59		T1	35	oC	s2b	1.1862	kg/s	Q_out	40.8865	kW
20	T_0	298.15	K	ssat.liq	1.3062		h1	245.805	kJ/kg						
21	P_0	101.325	kPa				v1	0.00076	m3/kg	Qevap_ORC	160.41	kW	W_total	10.3648	kW
22				hsat.vap	430.08		s1	1.1573		mf_ORC	0.22		η_overall	20.224	%
23				ssat.vap	1.7553								exg eff	58.3314	%
24															

Figure 12.15. The Excel sheet of the combined cycle using the input data of Ref. [15]

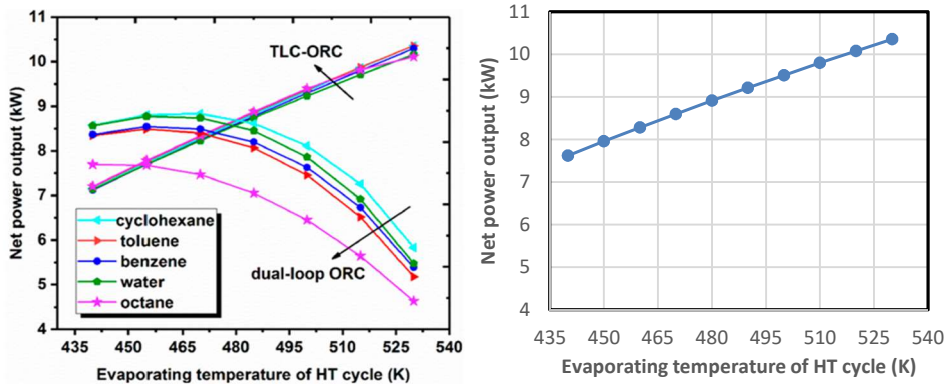

Figure 12.16. Comparison of the net power; (a) Ref. [15], (b) present cycle

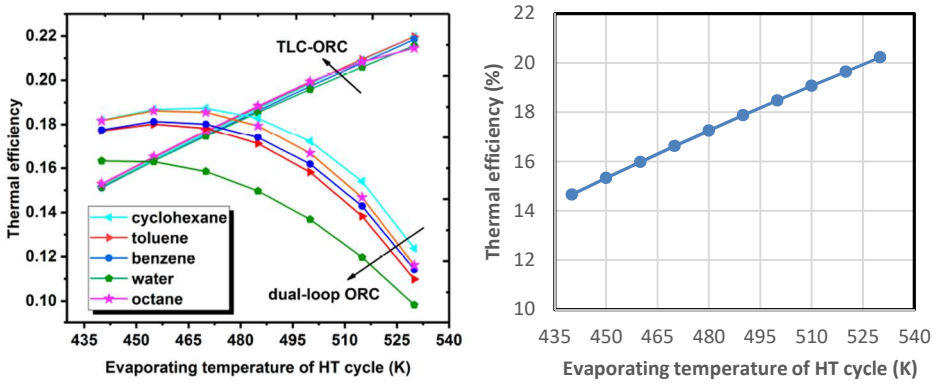

Figure 12.17. Comparison of the thermal efficiency; (a) Ref. [15], (b) present cycle

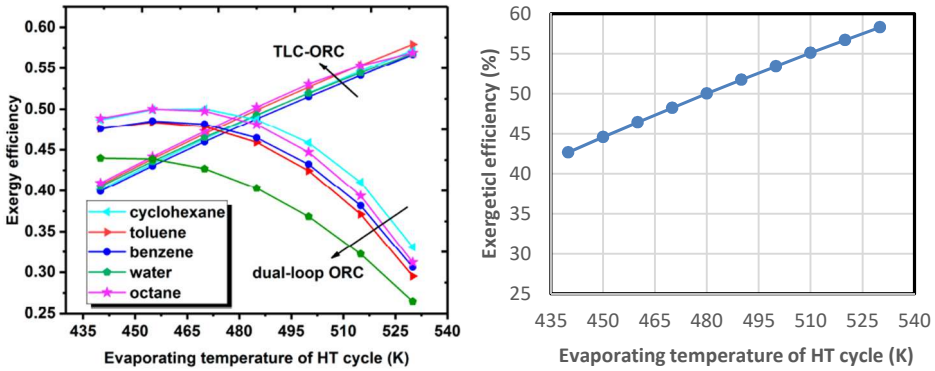

Figure 12.18. Comparison of the exergetic efficiency; (a) Ref. [15], (b) present cycle

Table 12.4 shows the exit temperature of the exhaust gas ($T_{hs,out}$) calculated by the present model at different values of the HT evaporator temperatures (T_{Evap_TFC}) together with the amount of heat recovered by the system ($\dot{Q}_{hs,Tot}$). The table also shows the corresponding amounts of heat recovered by the combined cycle of Ref. [15]. By allowing lower temperatures of the discharged gas, the present cycle could recover more energy and, therefore, produce more net power and give higher exergetic efficiencies than the cycle described by Yu et al [15]. However, reducing the average temperature of the heat-transfer process resulted in the lower thermal efficiencies.

Table 12.4. The heat recovered by the present cycle compared to that of Ref. [15]

T_{Evap_TFC} [K]	$T_{hs,out}$ [°C]	$\dot{Q}_{hs,Tot}$ [kW]	$\dot{Q}_{hs,Tot}$ [15] [kW]	Diff. (%)
440	67.142	52.005	45.87	13.375
470	68.351	51.735	45.83	12.885
500	69.469	51.485	45.78	12.462
530	70.517	51.251	45.69	12.171

12.6. Analysis of the combined cycle with five low-GWP fluids

The evaluation of the combined cycle presented in Section 12.4 did not take into consideration an important advantage of the combined cycle which is the allowance to use different working fluids in the TFC and ORC circuits. This section analyses the performance of the cycle for a heat source (hot pressurised water) at 120°C with five fluids that have zero ozone-layer depletion potential (ODP) and low global-warming potential (GWP), which are R152a, R1234yf, R600, R600a, and R717 [22].

12.6.1. Initial screening of the various fluid pairs

Figures 12.7 and 12.8 show that R1234yf can achieve the highest power and exergetic efficiency in the lower-temperature range, but it has the lowest thermal efficency. By using R1234yf in the ORC circuit and R152a in the TFC circuit, the model of the combined cycle was used to calculate the cycle's power and thermal efficiency at various temperatures in the cascade condenser. Figure 12.19 compares the values obtained by this pair with those of the simple ORC shown on Figures 12.7 and 12.8 and those of the

combined cycle with R152a in both circuits shown in Figure 12.11. Figure 12.19.a shows that both the power and thermal efficiency of the combined cycle with both fluid pairs are higher than those of the simple ORC at values of the cascade temperature below 80°C when the contribution of the TFC circuit is dominant. The figure also shows that the power of the combined cycle with the R152a/R1234yf pair remains higher than that of R152a in both circuits over the whole range of cascade temperatures, but Figure 12.19.b shows that the cycle's thermal efficiency with the R152a/R1234yf pair remains lower than that of R152a/R152a over the whole range of cascade temperatures. The model was also used to calculate the power and thermal efficiency of the combined cycle with the other three fluid pairs. The percentage deviations of the calculated values from those of the R152a/R1234yf pair are shown on Figure 12.20.

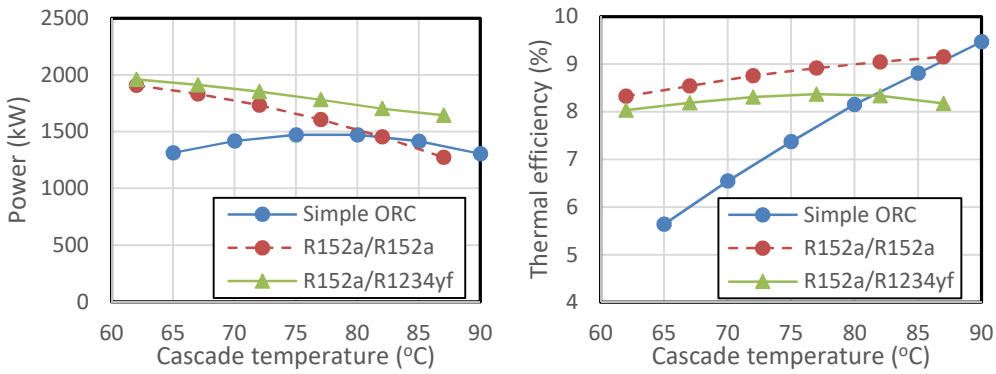

(a) (b)

Figure 12.19. Comparison of (a) the power and (b) thermal efficiency of the combined cycle with R152a/R1234yf with those with R152a/R152a and the simple ORC

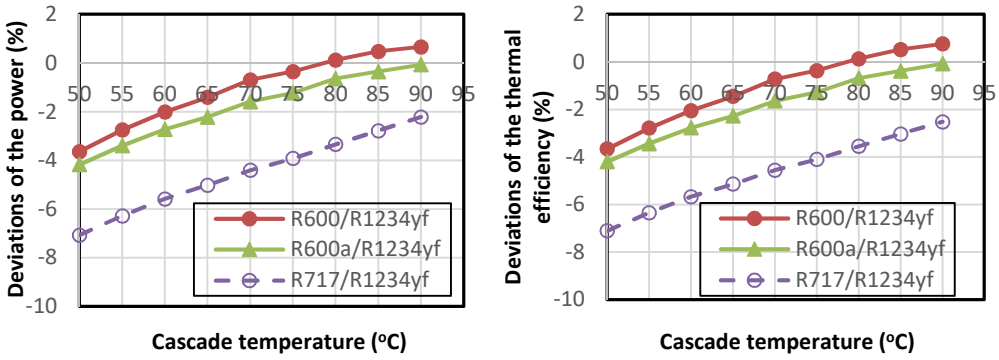

(a) (b)

Figure 12.20. Percentage deviations of (a) the power and (b) thermal efficiency of the combined cycle with R600, R600a, and R717 in the TFC circuit from those with R152a

Figure 12.20.a shows that all three pairs produce less power than R152a/R1234yf for cascade temperatures below 80°C, but the lowest values are those of the pair involving

R717. For all three fluid pairs, the deficits from the R152a/R1234yf pair diminish steadily as the cascade temperature is increased, but only R600/R1234yf manges to produce more power than R152a/R1234yf at temperatures above 80ºC. Figure 12.20.b shows that this also applies to the thermal efficiency since the thermal efficiency for each fluid pair deviates from the corresponding values of the R152a/R1234yf pair by the same pecentage as the pair's power. These results show that the two most favourable pairs for the combined cycle are R152a/R152a and R152a/R1234yf.

12.6.2. Tri-objective optimisation of the cycle with the most favourable pairs

This section compares the performance of the combined cycle with the two favourable fluid pairs at the cascade temperatures that gives the best trade-off between its power, thermal efficiency, and exergetic efficiency. Aiming to maximise the three performance indicators simultaneously is a multi-objective optimisation (MOO) problem. In general, MOO analyses of energy-conversion systems involve multiple factors such as the thermal efficiency and the economic and environmental factors. Excel's Solver can be used to perform single-objective optimisation (SOO) analyses, but not MOO analyses. Since the present analysis involves a single changing variable, which is the temperature in the cascade condenser, it can be conducted by using the free version of the MIDACO solver [19] that allows up to four changing variables to be considered. The set-up of MIDACO for this three-objective optimisation (3OO) analysis is shown on Figure 12.21.

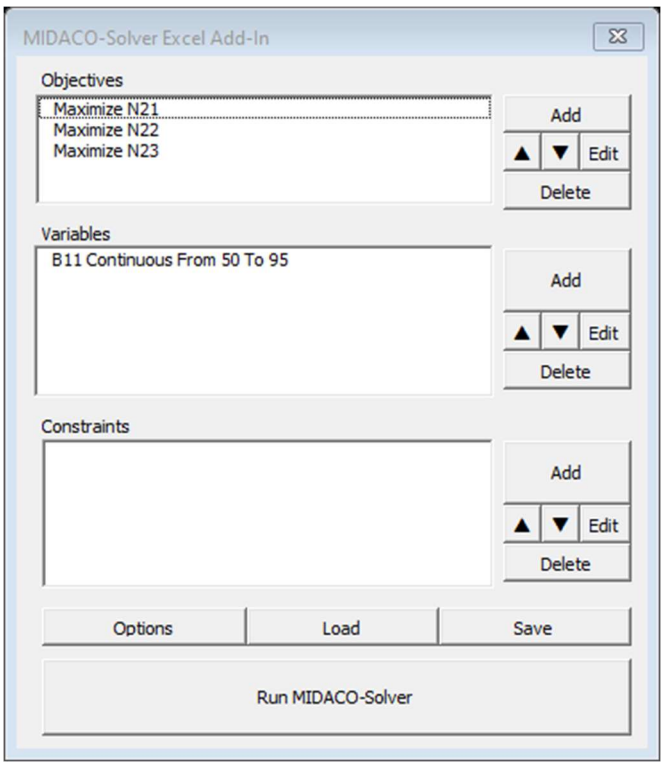

Figure 12.21. MIDACO's set-up for the 3OO analysis of the combined cycle

Figure 12.21 shows that three objective functions are involved in the analysis, which are the power, thermal efficiency, and exergetic efficiency of the combined cycle stored in cells N21, N22, and N23 of the model, respectively. All three objectives require the relevant performance parameter to be maximised by changing a single variable which is the cascade temperature of the TFC fluid stored in cell B10. Lower and upper limits are imposed on the temperature which are 50ºC and 95ºC, respectively. In general, MIDACO also allows constraints to be imposed on other cycle variables, such as the maximum allowable fluid pressure or flow rate, but this is not required in the present analysis. As an MOO solver, MIDACO generates a Pareto front that contains a set of un-dominated solutions from which one solution is selected. Figure 12.22 shows the solution selected by MIDACO with R152a as the single working fluid in both the TFC and ORC.

Pevap_TFC | =RefPsat_T(Fluid_TFC,Tevap_TFC)

	A	B	C	D	E	F	G	H	I	J	K	L	M	N	O
1	**Working fluids**			**TFC cycle**									**TFC**		
2	Fluid_TFC	R152a		T_hsi	82.83		s6	1.446641		h8	432.53072		Workt_TFC	1071.495	kW
3	Fluid_ORC	R152a					h7	439.22		s8	1.7122446		Workp_TFC	558.5776	kW
4	**Heating source (hot water)**			Pevap_TFC	4243.2		s7	1.7058					Worknet_TFC	512.9178	kW
5	T_hs	120	oC	Pcc_TFC	2008.326								Q_TFC	15774.73	kW
6	mflow	100	kg/s	h5	337.25223		ss8	1.7058					η_TFC	3.252	%
7	ρ	943.10	kg/m3	s5	1.4368662		xss8	0.452576							
8	cp	4.24	kJ/kg.K	mf_TFC	160.18105		hss8	430.301		s_hs	1.5279		**ORC**		
9	**TFC**			v5	0.0013263	m3/kg				s_0	0.3672		Q_sensible	65.98475	kJ/kg
10	Tevap_TFC	110	oC	h6	340.7394					Exerg_hs	4041.24		Q_ORC	4760.691	kW
11	Tcc_TFC	72.830523	oC	T6	74.432907								Workt_ORC	1364.762	kW
12	ΔTcc	3	K	**ORC cycle**									Workp_ORC	95.784	kW
13	ΔT_hs2	10	K	Tcc_ORC	69.830523	oC	s4s	2.035337		h2	272.6776		Worknet_ORC	1268.978	kW
14	**ORC**			Pcc_ORC	1879.4091	kPa	h4s	520.0802		T2	40.702639		η_ORC	6.338	%
15	Tcond_ORC	40	oC	Pcond_ORC	909.27	kPa	h4	523.4184		s2	1.2452456				
16	ΔT_sc	0.00	K				T4	40					**Overall parameters**		
17	ηt_isen	0.85		h3	542.33441		s4	2.045996		h2b	264.81596		Q_total	20535.42	kW
18	ηp_isen	0.85		s3	2.0353373					T2b	36.508379	kJ/kg	T_hsout	71.61	oC
19	ηx_isen	0.75		h2c	330.80071		T1	40	oC	s2b	1.2203994	kg/s	Q_out	18753.52	kW
20	T_0	298.15	K	s2c	1.4185831		h1	271.35	kJ/kg						
21	P_0	101.325	kPa				v1	0.001163	m3/kg	Qevap_ORC	211.5337	kW	W_total	1781.895	kW
22				h4b	531.28		s1	1.2411		mf_ORC	72.15	kW	η_overall	8.677	%
23				s4b	2.0711								ε_overall	44.0928	%
24															

Figure 12.22. Performance of the combined cycle with the tri-objective optimised solution obtained by MIDACO

Figure 12.22 shows the temperature of the cascade condenser determined by MIDACO, which is 72.74ºC. Figures 12.23 and 12.24 compare four cycle parameters of the 3OO optimised combined cycle with those of the ORC and TFC as shown on Table 12.2. Compared to the simple TFC, the optimised combined cycle reduced the power by 19.66%, but increased both the thermal efficiency and exergetic by 16.2%. and 13.54%, respectively. Compared to the simple ORC, the optimised cycle increased the power, thermal efficiency, and exergetic efficiency by 20.93%, 6.43%, and 70.92% respectively. The combined cycle has the highest thermal efficiency and exergetic efficiency. The 3OO solution for the combined cycle with the R152a/R1234yf pair was obtained following the same procedure described above. Table 12.5 compares the performance of the cycle with this optimised solution to those of the 3OO solution with R152a/R152a. The table figures show that the 3OO solution with R152a/R1234yf lowered the exit temperature of the heat source to 61.51ºC. The result is that the combined cycle produced more power, but with

less thermal and exergetic efficiencies compared to the cycle with R152a/R15a. Therefore, the comparison of the two fluid pairs to decide which one of them is favourable should take into considerations other factors such as the economic, safety, and environmental factors.

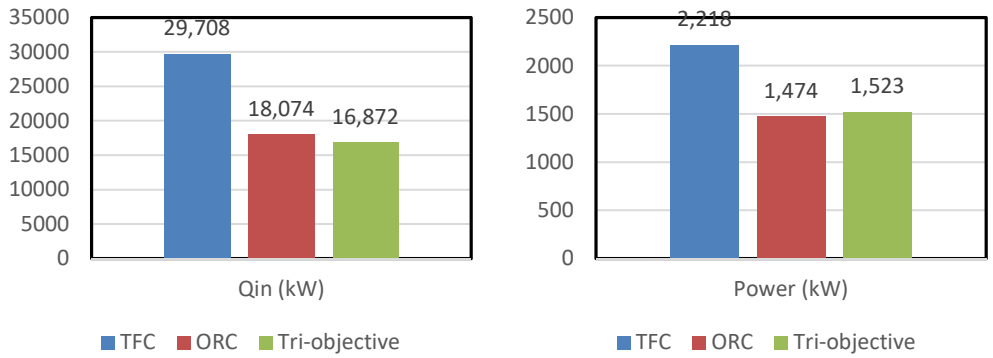

Figure 12.23. Comparison of the recovered heat and produced power by the optimised combined cycle with those of the simple TFC and ORC

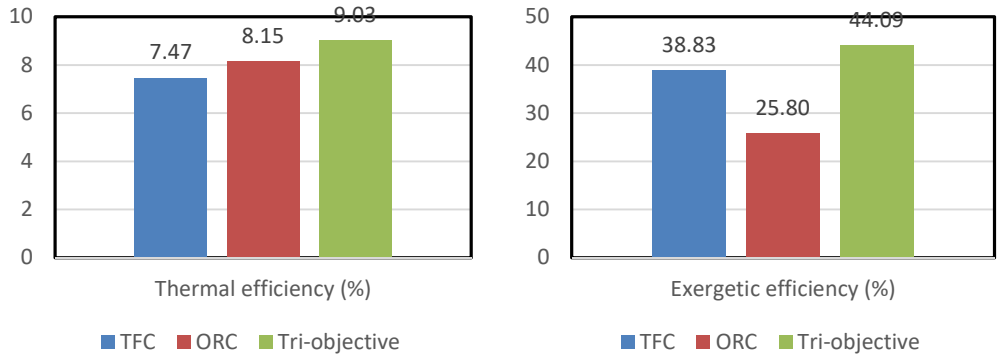

Figure 12.24. Comaprison of the thermal efficiency and exergetic efficiency of the optimised combined cycle with those of the simple TFC and ORC

Table 12.5. Thermodynamic parameters of the combined cycle at the two 3OO solutions using R152a/R152a and R152a/R1234yf

	3OO R152a/ R152a	3OO R152a/R1234yf
Ths,out (°C)	71.61	61.51
Qout (kW)	18753.52	22842.42
Qin (kW)	20535.42	24821.85
Power (kW)	1781.895	1979.427
Thermal efficiency (%)	8.677	7.975
Exergetic efficiency (%)	44.093	42.884

12.7. Closure

This chapter presents a combined cycle for power generation from low-grade heat sources that utilises the TFC in the high-temperature circuit and the ORC in the low-temperature circuits by connecting the two otherwise independent circuits via a casket condenser. The Excel-based model developed for analysing the cycle uses VBA functions to determine the thermodynamic properties of the working fluids. The accuracy of the VBA functions was checked by analysing the simple ORC and TFC as well as another combined ORC-TFC cycle and comparing the results with relevant published data for a number of suitable working fluids. Comparing the performance of the combined cycle for a heat source (hot pressurised water) available at 120°C to that of the simple ORC by using R152a in both cycles shows that the combined cycle gives more power and yields higher thermal and exergetic efficiencies than the simple ORC for cascade temperatures of 80°C and below. Compared to the simple TFC, the combined cycle generally produces less power, but achieves a higher thermal efficiency. The exergetic efficiency of the combined cycle is also higher than that of the simple TFC at a cascade temperature of 80°C. The performance of the cycle was also compared to that of the combined ORC-TFC described by Lu et al [15] for utilising the waste energy of an engine's exhaust gas available at 300°C. The results show that the net power produced and the thermal and exergetic efficiencies of the two cycles are comparable and that both cycles perform better than the conventional dual-loop ORC-ORC cycle. Finally, the performance of the combined cycle was analysed with four fluid pairs of low-GWP fluids that involve R1234yf in the ORC circuit and R152a, R600, R600a, or R717 in the TFC circuit. The results obtained at various values of the cascade temperature show that the most favourable fluid pairs for the cycle are those involving R152a, i.e., R152a/R152a and R152a/R1234yf.

Whether the same fluid or two different fluids are used in the two circuits of the combined cycle, the various analyses presented in the chapter show that its thermal efficiency steadily increases by increasing the temperature of the cascade condenser, but the power decreases while the exergetic efficiency has an optimum cascade temperature. Therefore, selecting the appropriate cascade temperature for the cycle requires a trade-off between its power, thermal efficiency, and exergetic efficiency. Tri-objective optimisation analyses of the cycle were conducted for the two pairs R152a/R152a and R152a/R1234yf that simultaneously maximised their three performance parameters. In general, the analyses with both fluid pairs show that the cycle keeps its advantages over the simple ORC and TFC, but they don't show a clear advantage of one pair over the other because the first pair produces more power while the second pair gives a higher thermal efficiency. Therefore, it is difficult to choose between the two pairs based on the thermo-dynamic performane alone. Determining which of the two fluid pair is more suitable and the appropriate cascade temperature requires other factors be taken into consideration such as the economic, safety, and environmental factors. In this respect, the Excel-based modelling platform allows multi-objective optimisation analyses to be conducted by using either the free version of the MIDACO solver or the Solver-TOPSIS technique described in [23].

References

[1] A.A. Bidgoli and J.I. Yanagihar, Integration of the Compression Units of the Processing Plant with an Organic Rankin Cycle for Power Generation and Cooling Process, Proceedings of ECOS 2023 - the 36th International Conference on Efficiency, Cost, Optimization, Simulation and Environmental Impact of Energy Systems 25-30 June, 2023, Las Palmas De Gran Canaria, Spain

[2] J.J. Fierro, C. Hern´andez-G´omez, C.A. Marenco-Porto, C. Nieto-Londo˜no, A. Escudero-Atehortua, M. Giraldo, H. Jouhara, L.C. Wrobel, Exergo-economic comparison of waste heat recovery cycles for a cement industry case study, Energy Conversion and Management: X 13 (2022) 100180

[3] C. Wolf, E. Rothuizen, T. Ommen, Exergoeconomic Analysis of a Solar Powered ORC using Zeotropic Mixtures for Combined Heat & Power Generation, Proceedings of ECOS 2023 - the 36th International Conference on Efficiency, Cost, Optimization, Simulation and Environmental Impact of Energy Systems 25-30 June, 2023, Las Palmas De Gran Canaria, Spain

[4] Forman, C., Muritala, I.K., Pardemann, R., Meyer, B. Estimating the Global Waste Heat Potential. Renew. Sustain. Energy Rev. 2016, 57, 1568–1579.

[5] Md Arbab Iqbal et al. Trilateral Flash Cycle (TFC): a promising thermodynamic cycle for low grade heat to power generation, 2nd International Conference on Energy and Power, ICEP2018, 13–15 December 2018, Sydney, Australia, / Energy Procedia 160 (2019) 208–214

[6] A. Skiadopoulos, C. Antonopoulou, K. Atsonios, P. Grammelis, A. Gkountas, P. Bakalis, G. Kosmadakis, and D. Manolakos, Trilateral Flash Cycle for efficient low temperature solar heat harvesting- A case study, Proceedings of ECOS 2023 - the 36th International Conference on Efficiency, Cost, Optimization, Simulation and Environmental Impact of Energy Systems 25-30 June, 2023, Las Palmas De Gran Canaria, Spain

[7] M. Yari, A.S. Mehr, V. Zare, S.M.S. Mahmoudi, M.A. Rosen, Exergoeconomic comparison of TLC (trilateral Rankine cycle), ORC (organic Rankine cycle) and Kalina cycle using a low grade heat source, Energy 83 (2015) 712-722

[8] K-Y. Lai, Y-T. Lee, M-R. Chen and Y-H. Liu, Comparison of the Trilateral Flash Cycle and Rankine Cycle with Organic Fluid Using the Pinch Point Temperature, Entropy (2019), 21, 1197

[9] P. Lykas, C. Antonopoulou, A. Gkountas, K. Atsonios, G. Itskos, N. Nikolopoulos, P. Grammelis, D. Manolakos and P. Bakalis, Thermodynamic and economic performance of novel organic cycle designs powered by low temperature waste heat, Proceedings of ECOS 2023 - the 36th International Conference on Efficiency, Cost, Optimization, Simulation and Environmental Impact of Energy Systems 25-30 June, 2023, Las Palmas De Gran Canaria, Spain

[10] L. Yu, W. Chen, A. Kan, Y. Zhang, S. Xue, J. Zeng, Investigation of a Dual-Loop ORC for the Waste Heat Recovery of a Marine Main Engine. Energies 2022, 15, 8365. https://doi.org/10.3390/en15228365

[11] X. Li, T. Liu and L. Chen, Thermodynamic Performance Analysis of an Improved Two-Stage Organic Rankine Cycle, Energies 2018, 11, 2864; doi:10.3390/en11112864

[12] Z.-Q. Wang, Y. Hu, X. Xia, Comparison of Conventional and Advanced Exergy Analysis for Dual-Loop Organic Rankine Cycle used in Engine Waste Heat Recovery, Journal of Thermal Science 30(1) 1-14, 2020 https://doi.org/10.1007/s11630-020-1299-x

[13] G. Liu, Q. Wang, J. Xu, Z. Miao. Exergy Analysis of Two-Stage Organic Rankine Cycle Power Generation System. Entropy 2021, 23, 43. https://doi.org/ 10.3390/e23010043

[14] Z. Li, R. Huang, Y. Lu, A. P. Roskilly, X. Yu, Analysis of a combined trilateral cycle - organic Rankine cycle (TLC-ORC) system for waste heat recovery, 10th International Conference on Applied Energy (ICAE2018), 22-25 August 2018, Hong Kong, China, Energy Procedia 158 (2019) 1786–1791, Science Direct, Available online at www.sciencedirect.com

[15] X. Yu, Z. Li, Y. Lu, R. Huang and A. P. Roskilly, Investigation of an Innovative Cascade Cycle Combining a Trilateral Cycle and an Organic Rankine Cycle (TLC-ORC) for Industry or Transport Application, Energies 2018, 11, 3032; doi:10.3390/en11113032, www.mdpi.com/journal/energies

[16] J.C. Jiménez-García, A. Ruiz, A. Pacheco-Reyes, W.A. Rivera, Comprehensive Review of Organic Rankine Cycles. Processes 2023, 11, 1982. https://doi.org/10.3390/pr11071982

[17] S. Trædal, Analysis of the Trilateral Flash Cycle for Power Production from Low Temperature Heat Sources. Master's Thesis, Institutt for Energi-og Prosessteknikk, Kolbjørn Hejes v 1B, Trondheim, 2014.

[18] C.O.C. Oko and, E.O. Diemuodeke, MS Excel spreadsheet add-in for thermodynamic properties and process simulation of R152a, Energy Science and Technology, Vol. 5, No. 2, 2013, pp. 63-69.

[19] M. Schlueter, J. Rueckmann, M. Gerdts. A Numerical Study of MIDACO on 100 MINLP Benchmarks, Optimization: A Journal of Mathematical Programming and Operations Research, 61,2012,7, 873-900.

[20] N.H. Mokarram, A.H. Mosaffa. Investigation of the thermoeconomic improvement of integrating enhanced geothermal single flash with transcritical organic Rankine cycle. Energy Convers. Manag. 2020, 213, 112831.

[21] M.J. Moran and H.N. Shapiro, Fundamentals of Engineering Thermodynamics, 5th edition, John Wiley, & Sons. Inc. 2006

[22] ASHRAE Handbook–Refrigeration, 2017, American Society of Heating, Refrigerating and Air-Conditioning Engineers, Inc., (SI Edition).

[23] M.M. El-Awad, A Solver-TOPSIS technique for multi-objective optimisation of innovative multi-stage VCR systems by using Microsoft Excel, Journal of Engineering Research. Faculty of Engineering-University of Tripoli, Issue (38), November 2024, 25-42, https://www.jer.ly/search_articles.php?f=38